Development 137, 2763-2772 (2010) doi:10.1242/dev.048108

Drosophila PAT1 is required for Kinesin-1 to transport cargo and to maximize its motility

Philippe Loiseau[1,*], Tim Davies[2,*], Lucy S. Williams[1], Masanori Mishima[2] and Isabel M. Palacios[1,†]

SUMMARY

Kinesin heavy chain (KHC), the force-generating component of Kinesin-1, is required for the localization of *oskar* mRNA and the anchoring of the nucleus in the *Drosophila* oocyte. These events are crucial for the establishment of the anterior-posterior and dorsal-ventral axes. KHC is also essential for the localization of Dynein and for all ooplasmic flows. Interestingly, oocytes without Kinesin light chain show no major defects in these KHC-dependent processes, suggesting that KHC binds its cargoes and is activated by a novel mechanism. Here, we shed new light on the molecular mechanism of Kinesin function in the germline. Using a combination of genetic, biochemical and motor-tracking studies, we show that PAT1, an APP-binding protein, interacts with Kinesin-1, functions in the transport of *oskar* mRNA and Dynein and is required for the efficient motility of KHC along microtubules. This work suggests that the role of PAT1 in cargo transport in the cell is linked to PAT1 function as a positive regulator of Kinesin motility.

KEY WORDS: Kinesin, Oocyte, Trafficking, *Drosophila*

INTRODUCTION

Kinesin-1 is composed of two heavy chains (KHC) and two light chains (KLC), which are encoded by single genes in *Drosophila melanogaster*. KHC has an N-terminal motor domain, a dimeric coiled-coil domain (stalk) and a globular C-terminal tail. KLC binds through its N-terminal heptad repeats (HRs) to coil 3 of the KHC stalk (amino acids 771-813 of human KHC; see Fig. S1A in the supplementary material) (Diefenbach et al., 1998), and its C-terminal region contains six tetra-trico-peptide repeat (TPR) motifs. The first cargoes identified to bind KLC through the TPR motifs were the c-Jun N-terminal kinase (JNK)-interacting proteins (JIPs) (Bowman et al., 2000; Gauger and Goldstein, 1993; Gindhart et al., 1998; Verhey et al., 2001). Since cargo binding is required for the activation of KHC, this finding implied that KLC is essential for Kinesin activity. However, KLC is not required for the association of all cargoes with Kinesin, suggesting that KHC activation and its binding to some cargoes rely on other mechanisms. For example, Milton binds KHC and attaches it to mitochondria in a KLC-independent manner (Rice and Gelfand, 2006).

In *Drosophila* oocytes, KHC is required for the localization of *oskar* mRNA to the posterior pole, an essential step in anterior-posterior axis formation. KHC is also required for the posterior localization of Dynein, for ooplasmic flows and for the anchoring of the nucleus to the anterior-dorsal corner of the oocyte, a crucial event in the determination of the dorsal-ventral axis. Surprisingly, in *Klc*-null mutants, ooplasmic streaming still occurs, both *oskar* mRNA and Dynein localize to the posterior and the nucleus is properly anchored (Brendza et al., 2000a; Brendza et al., 2002; Duncan and Warrior, 2002; Januschke et al., 2002; Palacios and St Johnston, 2002; Zimyanin et al., 2008). In these instances, it is not known how KHC recognizes its cargoes, or how its motor activity is regulated. This is also the case for the localization of the Fragile X mental retardation protein FMRP (also known as FMR1) and for glutamate receptor-interacting protein 1 (GRIP1), which are both reported to occur in a KLC-independent manner (Rice and Gelfand, 2006).

To understand the mechanism of KHC function in the *Drosophila* germline, we looked for candidate KHC regulators. Here we show that *Drosophila* Protein interacting with APP tail-1 (PAT1) (Zheng et al., 1998), a KLC-like protein, is required for the transport of several cargoes in the germline. The localization of *oskar* mRNA is aberrant in *Pat1* mutant oocytes, whereas the localization of Dynein, the position of the nucleus and ooplasmic flows seem normal. Interestingly, if the oocytes are mutant for both *Pat1* and *Klc*, Dynein is mislocalized to the anterior/lateral cortex and the *oskar* RNA mislocalization phenotype is more penetrant. PAT1 not only interacts genetically with Kinesin, but also biochemically, as shown by co-immunoprecipitation studies in various cellular extracts. These findings, together with the rescue of the *oskar* RNA phenotype in *Pat1* mutants by KLC overexpression, suggest that PAT1 and KLC act in a redundant manner, and explain why oocytes lacking KLC show no major defects in cargo transport. In addition, the velocity and run length of Kinesin are reduced in cell extracts that lack PAT1, suggesting that the requirement for PAT1 during Kinesin-1-mediated transport in the cell is a consequence of its function as a positive regulator of KHC motility.

MATERIALS AND METHODS

PAT1 sequence analysis and *Pat1* mutant alleles

The *Drosophila Pat1* gene (CG10695) is located on the X chromosome and encodes a predicted protein of 686 amino acids that shows 42% identity and 55% similarity with its human homolog. Structural analysis of the sequence (using Lasergene from DNAStar, Madison, WI, USA) shows that the protein is hydrophilic with no obvious signal sequence or membrane-spanning domains. As with human PAT1, *Drosophila* PAT1 shows homology to *Drosophila* KLC in the regions spanning the HR and TPR domains (see Fig. S1B in the supplementary material).

[1]The Zoology Department, University of Cambridge, Downing Street, Cambridge CB2 3EJ, UK. [2]The Gurdon Institute, University of Cambridge, Tennis Court Road, Cambridge CB2 1QN, UK.

*These authors contributed equally to this work
†Author for correspondence (mip22@cam.ac.uk)

Accepted 2 June 2010

We generated *Pat1* mutants by imprecise excision of the P element *P{EY15664}* inserted in the 5′UTR of *Pat1* (at position +37; see Fig. S1C in the supplementary material). PCR screening revealed a new *Pat1* allele with a 3.9 kb deletion within the gene, which was named *robin*. Antibodies against peptides from the N- and C-terminal regions of PAT1 did not recognize any fragments in *robin* oocyte extracts by western blot (see Fig. S1D in the supplementary material), indicating that no truncated proteins were produced. Furthermore, the same phenotypes were observed in $Pat1^{robin}$ females or in females that were $Pat1^{robin}/Df(ex)6240$, a deletion covering the *Pat1* genomic region, further supporting $Pat1^{robin}$ as a loss-of-function allele (data not shown).

Fly strains and germline clones

Fly stocks: *y,w,P{w+; mat-tub-a4:GFPstaufen},P{ry+;hs:FLP}* (Palacios and St Johnston, 2002); *w;P{w+; FRT}42B* Khc^{17} and w^{-}*;P{w+; FRT}42B* Khc^{23} (Serbus et al., 2005); *w;;P{w+; FRT}79D-F* Klc^{8ex94} (Gindhart et al., 1998); *P{EPgy2}Pat1EY*^{15664} and *PBac{RB}Pat1*^{e02477} (Bloomington Stock Center); *w,P{KZ503, Kin-β-Gal}* (Clark et al., 1994); *w,P{w+, mat-tub-a4:TauGFP]* (Micklem et al., 1997); *w;P{w+, GEN-KLC}* (Gindhart et al., 1998); *P{w+,ubiquitin promoter-c-myc-Khc+}* [generously provided by W. M. Saxton (Brendza et al., 2000b)]; *w;P{w+; mat-tub-a4:KHC(1-975)}*, *w;P{w+; mat-tub-a4:KHC(1-975)GFP}* and *w;P{w+; mat-tub-a4:KHC(1-849)-GFP}*. Germline clones were generated by the FLP system (Chou et al., 1993; Chou and Perrimon, 1996) using the lack of GFP as a marker for homozygous clones, or the Ovo^{D1} system, in which only homozygous mutant oocytes develop after stage 4 of oogenesis. Third instar larvae were heat shocked at 37°C for 2 hours for 3 consecutive days.

Molecular cloning

For transgenic fly strains, the *Drosophila* KHC region of interest (nucleotides 1-2925 for full-length and 1-2547 for tailless KHC) was cloned into pD277-GFP6 (van Eeden et al., 2001) to generate a construct in which the *α4-Tubulin* (*αTub67C*) promoter drives germline-specific expression of KHC fused to GFP6. Full-length KHC was also cloned into pD277 without GFP (Micklem et al., 1997). *Pat1* cDNA was amplified from the original pOT2 cDNA clone GH10889 and cloned into pD277, pD277-GFP6 and pUMAT-RFP (a gift from V. Mirouse, Clermont University France).

In situ hybridization and antibody staining

Immunostaining and RNA in situ hybridization were performed as described (Palacios and St Johnston, 2002). The following antibodies were used: rabbit Staufen (1:3000) (St Johnston et al., 1991), mouse β-galactosidase (1:200; Abcam), rabbit Oskar (1:500) (Markussen et al., 1995), mouse dynein intermediate chain (DIC) (1:1000; Chemicon), mouse P1H4 anti-DHC64C (1:200) (McGrail and Hays, 1997), β-actin (1:1000; AbCam) and monoclonal anti-Gurken (1:20; DHSB 1D12). All antibody stainings were performed using fluorescently labeled secondary antibodies (Jackson ImmunoResearch). PAT1 peptide antibodies against amino acids 149-164 and 671-686 were raised in rabbits (Eurogentec).

Cytoplasmic flow analysis

Analysis of cytoplasmic flows was performed as previously described (Palacios and St Johnston, 2002), except that images were taken using Leica SP5 confocal and DMI6000 inverted microscopes. Kalman images shown in Fig. 1D and Fig. S2 in the supplementary material were obtained by averaging eight successive scans into one composite image. The 'red' particles are uncharacterized vesicles, visualized by exciting the sample with 568 nm light.

Biochemical analyses

For immunoprecipitation of KHC dimers from oocytes (see Figs S3 and S4 in the supplementary material), *KHC(1-849)-GFP*, *KHC(1-849)-GFP;KHC-MYC* and *Pat1;;KHC(1-849)-GFP* females were fattened for 20 hours. Ovaries were dissected in PBT (PBS+0.1% Tween 20) and kept on ice. PBT was replaced with DIS buffer [25 mM Hepes pH 7.3, 50 mM KCl, 1 mM $MgCl_2$, 1 mM DTT, 0.1% NP40, EDTA-free Protease Inhibitors (Roche); 1:3 dry ovaries:buffer volume], and the ovaries homogenized on ice. After further diluting the homogenate with DIS buffer (1:1), the extracts were incubated with anti-GFP antibody (mouse, Invitrogen) and Protein A Sepharose CL-4B (GE Healthcare) for 3 hours. After binding, the immunoprecipitated complexes were washed four times with DIS containing 100 mM KCl. All steps were carried out at 4°C.

Drosophila S2 cells were grown at 25°C in Schneider's *Drosophila* Medium (Invitrogen) supplemented with 10% fetal bovine serum (Invitrogen) and penicillin-streptomycin (PAA Laboratories). Plasmids used were pIZM-V5 PAT1, pIZM-V5, pUAS-KHC(1-849)-GFP, pUAS-GFP, pUAS-MYC-KLC and pMT-GAL4 (KLC, PAT1 and KHC refer to *Drosophila* cDNAs). Cells were incubated with medium, Cellfectin II (Invitrogen) and the relevant DNAs for 20 hours, after which the mix was replaced with pure medium. Five hours later, the expression of proteins was induced by adding $CuSO_4$ to 100 μM. Cells were then harvested and lyzed using the lysis buffer provided with the GFP-Trap-A Kit (Chromotek). Immunoprecipitations were carried out as specified for the KHC immunoprecipitations from oocyte extracts. Antibodies used for immunoprecipitations were mouse anti-GFP (Invitrogen), mouse anti-V5 (Invitrogen) and mouse anti-c-Myc (Cell Signaling). Antibodies used for western blotting were mouse anti-V5 (1:5000; Invitrogen), mouse anti-c-Myc (1:3000; Cell Signaling) and mouse anti-GFP (1:3000; Clonetech).

Imaging of Kinesin-GFP movement with total internal reflection fluorescence (TIRF) microscopy

This assay was modified from studies on the movement of endosomes (Hoepfner et al., 2005; Nielsen et al., 1999). Microscope chambers with Taxol-stabilized microtubules immobilized on a coverglass surface were prepared as previously reported (Helenius et al., 2006), except that ultracleaned coverglasses (ThermoFisher Scientific, Portsmouth, NH, USA) were treated with Sigmacote (Sigma). For preparation of extracts, ~30 ovaries were homogenized in BRB80 buffer (80 mM Pipes pH 6.9, 1 mM $MgCl_2$, 1 mM EGTA, 50 mM KCl and Protease Inhibitors; 1:2 dry ovaries:buffer volume) and kept on ice until use. For motility assays, 17.5 μl of BRB20-Taxol solution (20 mM Pipes, 1 mM $MgCl_2$, 1 mM EGTA, 20 μM Taxol) was added to 3 μl of the ovary extracts supplemented with 50 μg/ml casein, 1 mM ATP and oxygen scavenger mix (0.25 μl β-mercaptoethanol, 100 mM D-glucose, 0.4 mg/ml glucose oxidase, 50 μg/ml catalase) and perfused into the flow cell. Images were acquired and analyzed as previously reported (Hutterer et al., 2009). The velocity and diffusion coefficient were calculated for each trajectory by plotting the mean square displacement (MSD) against time and fitting to the curve $MSD=v^2t^2+2Dt$. The MSD was calculated using the position of the particles at each time point during interaction with the microtubule. This allowed the velocity and diffusion components of one-dimensional movement to be determined. Trajectories that showed moderately unidirectional motility [v/D between 10^{-5} and 10^{-1} nm^{-1}; fitting correlation coefficient greater than 0.95; gap in trajectory less than 40%; no outliers (greater than four times the s.d.) in displacements in 100 mseconds] were statistically analyzed.

RESULTS

PAT1 is required for *oskar* mRNA localization

PAT1, a KLC-like protein with five HRs and four imperfect TPR motifs, was first identified in human cells (where it is now known as APPBP2), in which it interacts with the basolateral sorting signal of APP (Kuan et al., 2006; Zheng et al., 1998). *Drosophila* PAT1 also shows homology to KLC in the regions spanning the HR and TPR domains (see Fig. S1B in the supplementary material). To test whether PAT1 is required for KHC function, we studied the localization of *oskar* mRNA in *Pat1* mutant ovaries. In contrast to wild-type stage 9 oocytes, in which the transcript is localized in a posterior crescent, *oskar* mRNA and Staufen, a marker for the transcript, were found in an ectopic region in 22% (n=40) and 25% (n=140) of *Pat1* mutant oocytes, respectively (Fig. 1A-C; see Fig. 3C). Other KHC-dependent processes in the oocyte, such as the localization of Dynein and nucleus anchoring, were not affected in *Pat1* mutants (Fig. 1B,C). Similarly, ooplasmic streaming was still

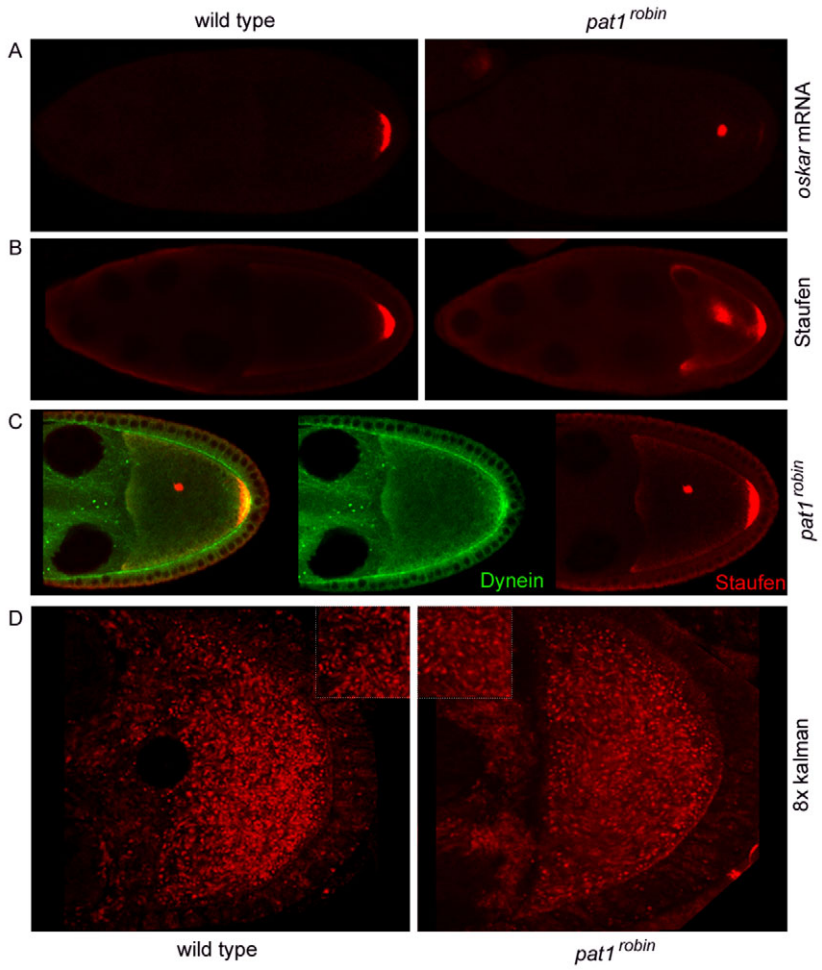

Fig. 1. PAT1 is required for *oskar* mRNA localization, but not for Dynein transport or cytoplasmic flows. (**A**) In situ hybridization for *oskar* mRNA at stage 9 of oogenesis in wild-type (left) and *Pat1* mutant (right) *Drosophila* ovaries. In wild-type egg chambers, *oskar* mRNA localizes to the posterior pole of the oocyte, where it remains anchored throughout oogenesis. This localization is impaired in *Pat1* mutant ovaries. Ectopic dots of *oskar* mRNA are found in 22% of *Pat1* stage 9 oocytes (n=40), but in only 7% of wild-type oocytes (n=40). (**B**) Staufen protein (a marker for *oskar* mRNA) in wild-type (left) and *Pat1* mutant (right) stage 9 egg chambers. As with *oskar* mRNA, Staufen is found in an ectopic region in 25% of the *Pat1* oocytes (n=140; see Fig. 3). (**C**) Dynein heavy chain (green) and Staufen (red) in stage 9 *Pat1* oocytes. Unlike Staufen, Dynein is not found as a dot in *Pat1* mutants. (**D**) Particles that reflect 568 nm light ('red' particles) in wild-type (left) and *Pat1* mutant (right) egg chambers. Each image results from a continuous confocal scan, averaged eight times using the Kalman function. Insets show representative streaks of dots, which are used as a qualitative measure of cytoplasmic streaming.

detectable in the absence of PAT1, showing that PAT1 is not absolutely required for these flows (Fig. 1D; see Fig. S2 in the supplementary material).

In wild-type stage 9 oocytes, *oskar* RNA is localized to the posterior pole, where it is anchored throughout the rest of oogenesis. It is possible, therefore, that the mislocalization of *oskar* RNA in *Pat1* mutants is a consequence of PAT1 acting on the anchoring of *oskar* at the cortex. However, only 12.3% (n=61) of late *Pat1* mutant oocytes (stage 11) presented an ectopic Staufen mislocalization, in contrast to 25% (n=140) of stage 9 *Pat1* oocytes (P<0.0375 by Fisher's test). This observation suggests that the anchoring of *oskar* mRNA at the posterior is unaffected in *Pat1* oocytes. The *oskar* mRNA and Staufen localization defects in *Pat1* females were rescued by the germline-specific expression of *Pat1* cDNA (see Table S1 in the supplementary material), showing that PAT1 is required in the germline for the KHC-dependent transport of *oskar* mRNA to the posterior pole.

PAT1 is not required for microtubule organization or regulation of Oskar translation

The *oskar* mRNA localization defects observed in *Pat1* mutants resemble the phenotype described for *oskar*-overexpressing oocytes, in which premature translation of Oskar protein results in the mislocalization of *oskar* RNA to an ectopic region (Zimyanin et al., 2007). To investigate whether the *oskar* mislocalization phenotype in *Pat1* mutants is due to the premature translation of *oskar*, we analyzed the temporal regulation of *oskar* translation in wild-type and *Pat1* mutant oocytes. In wild-type egg chambers, Oskar protein was not detected at stage 8 of oogenesis, and started accumulating at stage 9 (Fig. 2A). Similarly, the translation of *oskar* RNA did not take place in early *Pat1* oocytes, and Oskar was only detected from stage 9 (Fig. 2A). We conclude that the mislocalization of *oskar* mRNA in *Pat1* mutants is not due to its premature translation.

Neither the accumulation of Dynein at the posterior of the oocyte, nor the Dynein-dependent transport of the nucleus, was affected in *Pat1* mutants, suggesting that PAT1 is not required for the organization of microtubules. To further test this, we analyzed the distribution of both Kin-β-Gal and the microtubule-binding protein Tau in wild-type and *Pat1* oocytes. A GFP-tagged version of Tau showed that the overall morphology of the microtubules was not affected in *Pat1* mutants (Fig. 2C). Kin-β-Gal is a fusion of β-galactosidase to amino acids 1-604 of KHC and, as with endogenous KHC, localizes to the posterior in wild-type oocytes (Brendza et al., 2002; Clark et al., 1994; Duncan and Warrior, 2002; Januschke et al., 2002; Palacios and St Johnston, 2002). This localization of Kin-β-Gal to the posterior pole is affected when cytoskeletal polarity is disrupted. However, the localization of Kin-β-Gal was normal in *Pat1* oocytes, where it was found at the posterior, and not in the ectopic Staufen-containing dots (Fig. 2E). In addition, *bicoid* RNA and Gurken protein always showed a wild-type localization to the anterior cortex and anterior-dorsal corner, respectively (Fig. 2B,D). Thus, the Dynein-dependent localization of RNAs and the polarization of the microtubule cytoskeleton are not disrupted in *Pat1* mutant oocytes.

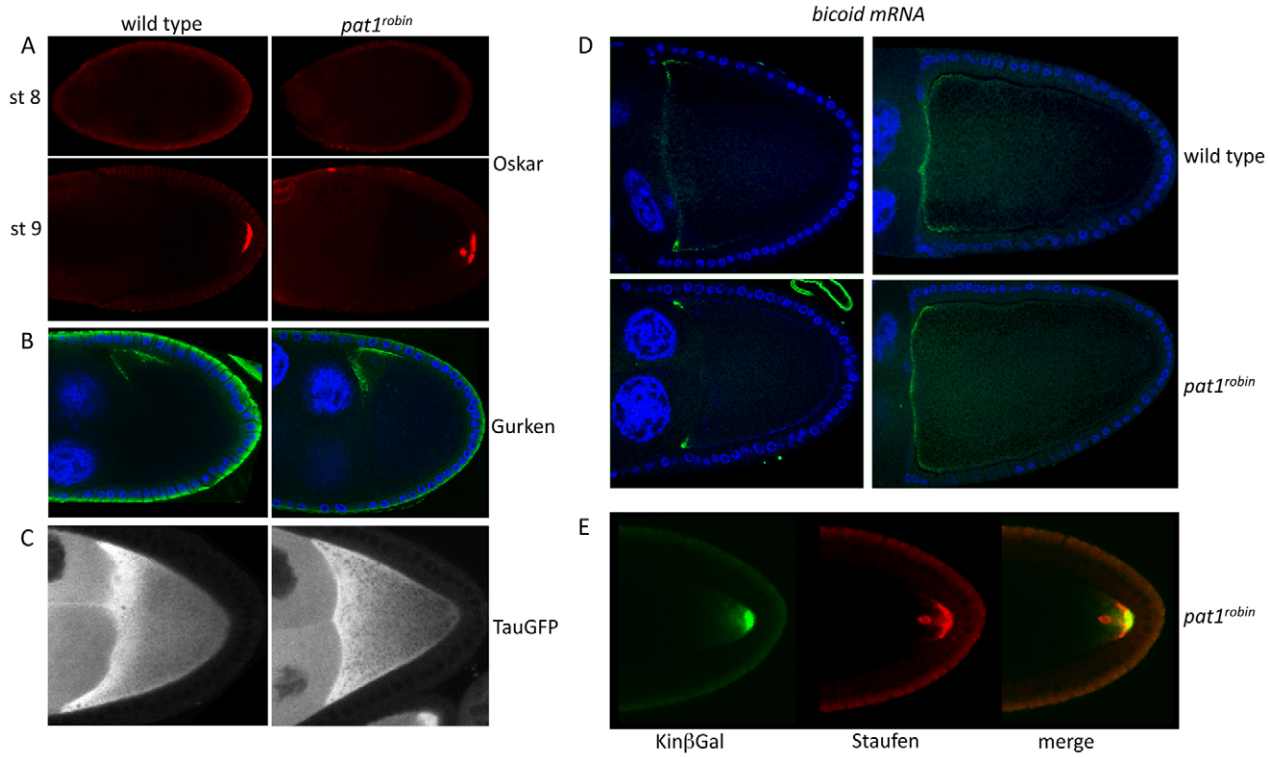

Fig. 2. PAT1 is not required for microtubule organization or regulation of Oskar translation. (**A**) Oskar protein (red) in stage 8 (top) and stage 9 (bottom) wild-type (left) and *Pat1* (right) *Drosophila* egg chambers. In wild-type and *Pat1* ovaries, Oskar protein is not detected at stage 8 of oogenesis, but starts accumulating at stage 9. (**B**) Gurken protein localizes normally to the anterior-dorsal corner in stage 9 wild-type (left) and *Pat1* mutant (right) oocytes. (**C**) Tau-GFP labeling of microtubules in living wild-type (left) and *Pat1* mutant (right) stage 9 oocytes. The overall organization of the microtubule cytoskeleton appears normal in *Pat1* oocytes. (**D**) In situ hybridization for *bicoid* mRNA in wild-type (top) and *Pat1* mutant (bottom), stage 9 (left) and stage 10b (right) oocytes. *bicoid* mRNA localization to the anterior pole is not affected by *Pat1* loss of function. (**E**) Kinesin-β-galactosidase (KinβGal, green) and Staufen (red) in *Pat1* mutant oocytes. Unlike Staufen, Kinesin-β-galactosidase localizes only to the posterior pole of *Pat1* oocytes.

PAT1 and KLC interact genetically to affect the transport of some cargoes

Since PAT1 is a KLC-like protein and *oskar* mRNA is mislocalized in only 22% of *Pat1* mutants, we hypothesized that PAT1 and KLC might act redundantly in the transport of *oskar* mRNA. To test this, we analyzed the localization of Staufen in *Pat1, Klc* double-mutant egg chambers. As in *Pat1* mutants, Staufen was mislocalized to an ectopic region in the posterior half of *Pat1, Klc* double-mutant oocytes (Fig. 3A,B). However, this phenotype was observed in 78.1% of the *Pat1, Klc* egg chambers, representing over three times the penetrance of the single-mutant phenotypes (Fig. 3C).

To study whether this genetic interaction between PAT1 and KLC applies to other cargoes of KHC, we analyzed the localization of the nucleus and Dynein in *Pat1, Klc* oocytes. Although the nucleus was always anchored at the anterior corner in the double-mutant oocytes, Dynein did not localize to the posterior in these egg chambers and was instead found at the anterior/lateral cortex (Fig. 3B).

These results indicate that PAT1 and KLC have a functional interaction in the localization of *oskar* mRNA and Dynein to the posterior of the oocyte. This genetic interaction between PAT1 and KLC, together with their sequence homology, raises the possibility that PAT1 and KLC might act in a redundant manner in the localization of cargoes in the germline. To study this hypothesis further, we increased the KLC dosage by expressing a full-length KLC-encoding transgene (Gindhart et al., 1998) in *Pat1* mutant oocytes. The Staufen mislocalization phenotype was fully rescued in these flies (see Table S1 in the supplementary material).

Pat1 mutants enhance the defects caused by a mutant form of KHC

To study whether PAT1 interacts functionally not only with KLC but also with KHC, we analyzed the effects of mutating *Pat1* in egg chambers that express a mutant form of KHC. Expression of a truncated KHC that is missing the last 125 amino acids and fused to GFP [KHC(1-849) or 'tailless'; see Fig. S1A in the supplementary material) induced the mislocalization of Staufen in 18% of the oocytes [KHC(1-849)-GFP/+, n=50; Fig. 4]. This effect on the localization of Staufen was specific for this tailless KHC, as the expression of full-length KHC showed no defects (n=20; Fig. 4A). How KHC(1-849) acts as a mutant form of KHC is not fully understood, but this truncated KHC was able to both efficiently dimerize with endogenous KHC and localize to the posterior pole (Fig. 4A; see Figs S3 and S4 in the supplementary material). Furthermore, a reduction of KHC dosage enhanced the Staufen mislocalization phenotype in flies expressing tailless KHC, whereas an increase in the KHC dosage reduced the Staufen phenotype (see Table S2 in the supplementary material). These observations suggest that KHC(1-849) might act as a mutant motor by titrating out full-length KHC, so reducing the number of *oskar*-

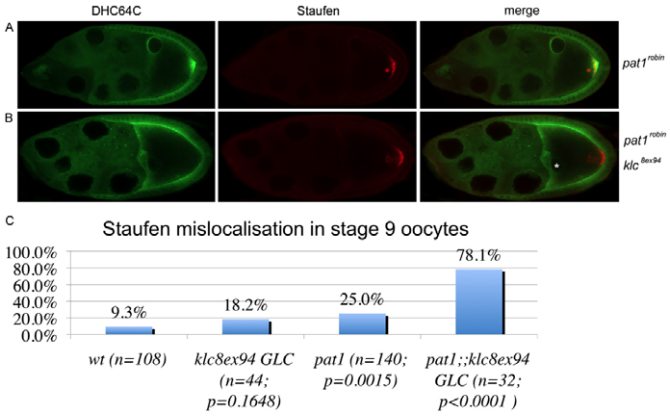

Fig. 3. PAT1 and KLC interact genetically. (**A**) Dynein (green) and Staufen (red) in stage 9 *Pat1* egg chambers. Unlike Staufen, Dynein is not mislocalized in *Pat1* mutant egg chambers. (**B**) Dynein (green) and Staufen (red) in stage 9 *Pat1, Klc* oocytes. In these double mutants, Dynein is mislocalized at the anterior/lateral cortex. The *Pat1, Klc* double-mutant oocytes were obtained by inducing Klc^{8ex94} germline clones in a $Pat1^{robin}$ mutant background. Note that the oocyte nucleus (asterisk) is not mislocalized in this double-mutant background, and it only seems so because of the orientation of the egg chamber, with its anterior-dorsal corner towards the observer. (**C**) Quantification of the Staufen mislocalization phenotype in stage 9 wild-type egg chambers, *Klc* germline clones (Klc^{8ex94} GLC), *Pat1* mutants and *Pat1, Klc* (*Pat1*;;Klc^{8ex94} GLC) double mutants. Although Staufen mislocalization is not statistically different between *Klc* and wild-type egg chambers (P=0.16, Fisher's exact test), it is significantly higher in *Pat1* mutants compared with wild type (P=0.0015, Fisher's exact test). The penetrance of the Staufen mislocalization phenotype is dramatically increased (by more than threefold) in *Pat1, Klc* double mutants compared with single *Pat1* or *Klc* mutants, which demonstrates that *Pat1* and *Klc* interact genetically (P<0.0001, Fisher's exact test). The mislocalization of Staufen to a dot in the center of the oocyte was never found in wild-type flies, although dots closely attached to the posterior crescent were occasionally observed and included in the quantification.

localizing, functional KHC dimers. In tailless KHC-expressing ovaries where the endogenous KHC dosage is reduced, fewer KHC dimers that can fully support *oskar* localization would be formed, and the phenotype would consequently be enhanced. Ovaries that express KHC(1-849) and a higher dosage of full-length KHC would have more functional motor dimers and show a partial rescue of the *oskar* phenotype.

When KHC(1-849)-GFP was expressed in *Pat1* mutants, the mislocalization of Staufen was not only more pronounced (Fig. 4A), but was also observed in 80% of the egg chambers, which is over four times the penetrance of the Staufen phenotype in KHC(1-849)-GFP/+ ovaries (n=38; Fig. 4B). This result shows that the loss of function of *Pat1* enhances the *oskar* RNA localization defects caused by this mutant form of KHC, suggesting that PAT1 and tailless KHC somehow affect the same pathway of *oskar* localization.

PAT1 associates with Kinesin-1

To study whether PAT1 associates with Kinesin, we performed biochemical interaction studies. Since the quality of the KLC and PAT1 antibodies was not sufficient in our hands for interaction studies in oocyte extracts, we used MYC-tagged KLC, V5-tagged PAT1, and KHC(1-849)-GFP for immunoprecipitation experiments using cultured *Drosophila* cells. Endogenous KHC and KLC-MYC specifically co-purified with PAT1 when PAT1-V5 was immunoprecipitated using an anti-V5 antibody. As a control, the immunoprecipitation was performed with extracts that expressed empty V5, instead of PAT1-V5. The PAT1-KLC interaction was validated by performing similar pull-downs in the reverse direction, using cells that expressed KLC-MYC and PAT1-V5 (Fig. 5B). In this case, PAT1-V5 specifically co-purified with KLC-MYC using an anti-MYC antibody.

PAT1 has a strong functional interaction with the truncated KHC(1-849) protein. To study whether PAT1 associates with this tailless KHC, we immunoprecipitated KHC(1-849)-GFP by its GFP tag from cells that expressed PAT1-V5. As shown in Fig. 5C, PAT1 specifically co-purified with KHC(1-849)-GFP. As a control, we performed the same immunoprecipitation with extracts that expressed PAT1-V5 with GFP alone. The interaction of tailless KHC-PAT1 was validated by performing similar pull-downs in the reverse direction, using cells that expressed KHC(1-849)-GFP and either PAT1-V5 or empty V5 (Fig. 5D). KHC(1-849)-GFP specifically co-purified with PAT1 when PAT1-V5 was immunoprecipitated using an anti-V5 antibody.

These results show that PAT1 forms a complex with KHC in a tail-independent manner, similarly to the known interaction between KHC and mammalian KLC (Diefenbach et al., 1998). To study whether *Drosophila* KLC also binds tailless KHC, we immunoprecipitated KLC-MYC from cells expressing KHC(1-849)-GFP. The KLC-binding domain was still present in tailless KHC and the Kinesin-1 complex was able to form (see Fig. S5 in the supplementary material).

Together, these results show that PAT1 forms a complex with Kinesin-1, and that this association between PAT1 and the motor does not require the tail domain of KHC. Whether this interaction is direct or is mediated by additional factors needs further study.

The velocity and run length of Kinesin are reduced in the absence of *Pat1*

As PAT1 interacts both biochemically and genetically with Kinesin, it is likely that the aberrant localization of *oskar* mRNA in *Pat1* oocytes is due to defects in the transport of the transcript. If this is the case, what is the possible molecular mechanism of PAT1 function in *oskar* transport? The ectopic accumulation of *oskar* mRNA in *Pat1* mutants partially resembles the *oskar* phenotype in Khc^{17} mutant oocytes (see Fig. S6 in the supplementary material) (Serbus et al., 2005). Khc^{17} is a hypomorphic allele caused by a missense mutation in the motor domain (S246F) that reduces the ATPase activity and velocity of KHC (Brendza et al., 1999). When we analyzed in detail the Staufen phenotype in Khc^{17} oocytes, we noticed that Staufen was distributed ectopically in a diffuse manner, as previously described (Serbus et al., 2005), but also in dot-like structures, similar to those found in *Pat1* mutants (see Fig. S6 in the supplementary material). Also, similarly to *Pat1*, Khc^{17} enhanced the Staufen phenotype fivefold in KHC(1-849)-expressing ovaries (see Fig. S6 in the supplementary material). Whether this mislocalization of *oskar* RNA in Khc^{17} oocytes is linked to the slower motility of KHC or to some other property of the mutant motor is unknown, but the transcript is transported more slowly in this mutant (Zimyanin et al., 2007). Furthermore, a similar phenotype is observed in oocytes that are mutant for the Khc^{23} allele, a mutation that also results in a slower motor and slowed *oskar* RNA transport (see Fig. S6 in the supplementary material) (Serbus et al., 2005; Zimyanin et al., 2007).

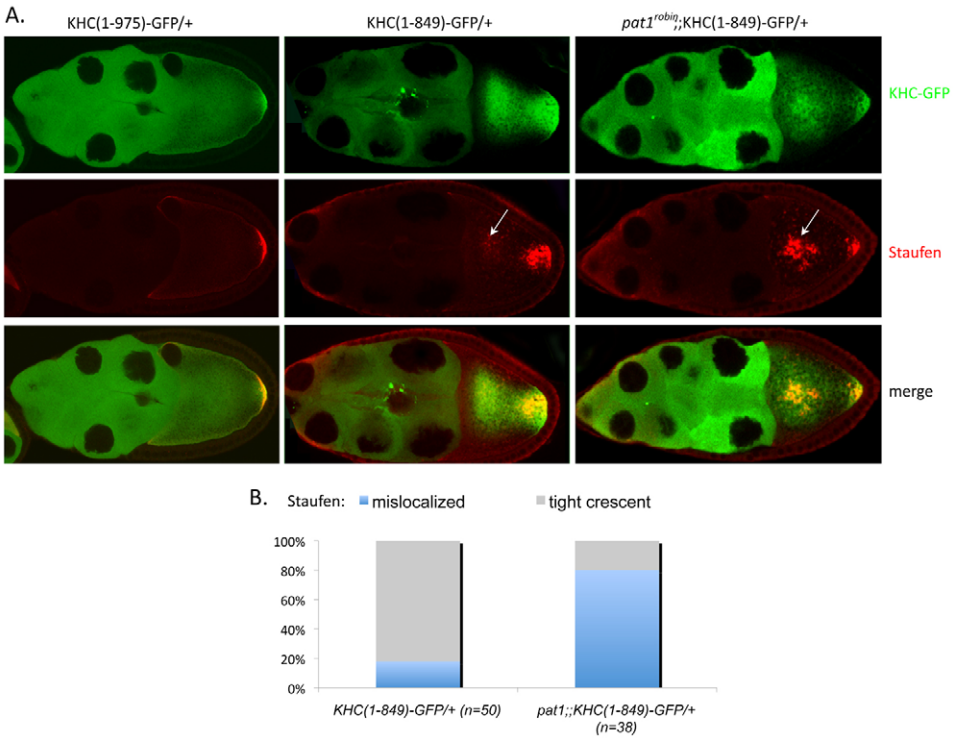

Fig. 4. Loss of function of *Pat1* enhances the phenotype of a mutant form of KHC. (**A**) Staufen (red) in *Drosophila* egg chambers that express one copy of KHC(1-975)-GFP (left), one copy of KHC(1-849)-GFP (middle), or one copy of KHC(1-849)-GFP but are also mutant for *Pat1* (right). Top panels show the localization of the various KHC-GFP fusions. In contrast to oocytes expressing the full-length KHC, Staufen (red) is mislocalized in 18% of the KHC(1-849)-GFP-expressing oocytes (see B). This mislocalization is more severe and four times more penetrant in *Pat1*^{robin};;KHC(1-849)-GFP oocytes than in the KHC(1-849)-GFP-expressing egg chambers. Arrows point to the region where Staufen is mislocalized. (**B**) Quantification of the Staufen mislocalization phenotype in stage 9 egg chambers that express one copy of tailless KHC fused to GFP, and that are either wild-type [KHC(1-849)-GFP/+] or mutant for *Pat1* [*Pat1*;;KHC(1-849)-GFP/+].

To explore whether PAT1 has an effect on the velocity of Kinesin, we set up an in vitro assay to analyze the movement of KHC-GFP along microtubules in ovary extracts using total internal reflection fluorescence (TIRF) microscopy (Fig. 6A). A comparison of the behavior of Kinesin between control and *Pat1* mutant extracts would address the effect of PAT1 on the motility of the motor, regardless of the details of the PAT1-KHC interaction.

First, we sought a KHC-GFP construct suitable for single-molecule analyses. Full-length KHC-GFP did not show frequent processive movement (data not shown), presumably owing to the C-terminal autoinhibitory domain (Coy et al., 1999; Friedman and Vale, 1999), and did not allow statistically reliable measurements of its motility. Conversely, KHC(1-849)-GFP showed slightly diffusive, but mostly unidirectional and processive movement along microtubules (Fig. 6B; see Movies 1 and 2 in the

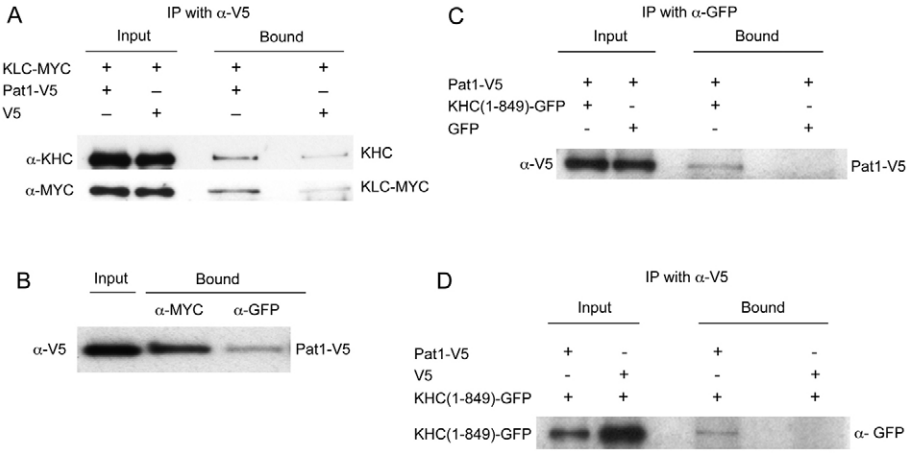

Fig. 5. PAT1 interacts with Kinesin-1. (**A**) *Drosophila* S2 cells co-expressing KLC-MYC and either PAT1-V5 or empty V5 were immunoprecipitated with an anti-V5 antibody (α-V5). Endogenous KHC (top) and KLC-MYC (bottom) were specifically co-purified with PAT1. (**B**) *Drosophila* S2 cells expressing PAT1-V5 and KLC-MYC were immunoprecipitated using an anti-MYC antibody (α-MYC) or an unrelated antibody (α-GFP) as a control. PAT1 is specifically co-immunoprecipitated with KLC-MYC by the anti-MYC antibody. (**C**) *Drosophila* S2 cells expressing PAT1-V5 and either KHC(1-849)-GFP or GFP alone were immunoprecipitated using anti-GFP antibody. PAT1-V5 is specifically pulled down by the anti-GFP antibody when KHC(1-849)GFP is present, indicating that PAT1 is in a complex with tailless KHC. (**D**) *Drosophila* S2 cells expressing KHC(1-849)-GFP and either PAT1-V5 or V5 alone were immunoprecipitated using anti-V5 antibody. KHC(1-849)-GFP is specifically pulled down by the anti-V5 antibody when PAT1-V5 is present, indicating that tailless KHC is in a complex with PAT1. Note that the expression of KHC(1-849)-GFP in cells transformed with the empty V5 plasmid is higher than in cells expressing PAT1-V5 (the amount of extract loaded in each input was the same). Each immunoprecipitation was performed in triplicate. Representative blots are shown.

supplementary material). Although this construct lacks the autoinhibitory domain, it still contains the KLC-binding domain (see Introduction and Fig. S5 in the supplementary material). It is important to note that these ovaries express endogenous KHC and the GFP-tagged tailless KHC, and that these two forms of the motor can dimerize with each other (see Figs S3 and S4 in the supplementary material). As a consequence, the GFP particles might represent homodimers of the truncated KHC or heterodimers of tailless KHC with endogenous KHC. However, the effect of this heterogeneity should be equivalent in the control and *Pat1* extracts, as PAT1 does not seem to affect expression of the endogenous KHC or the transgene, and the dimerization state of the truncated motor with endogenous KHC was also similar in control and *Pat1* mutant extracts (see Fig. S3 in the supplementary material). Importantly, *Pat1* enhances the *oskar* RNA localization phenotype observed in ovaries expressing tailless KHC (Fig. 4). Therefore, any difference detected in the motility of this truncated KHC between the control and *Pat1* mutant can be related to the role of PAT1 in vivo.

We compared the motility of KHC(1-849)-GFP in control and *Pat1* extracts by automated tracking of the GFP signals along immobilized microtubules (Fig. 6C-E). In addition to measuring the duration and distance of individual processive runs (association time and run length), we analyzed particle velocity. This was achieved by assuming that processive runs consist of directional movement (with velocity v) and diffusive movement (with diffusion coefficient D) along the microtubule. Velocity and diffusion of a particle are then determined by fitting the mean square displacement (MSD) of a particle to the form $MSD(t)=v^2t^2+2Dt$ (Okada and Hirokawa, 1999). In control extracts, the average of the velocities determined for individual particles was ~340 nm/second (337±8 nm/second, n=285), which is slightly lower than the velocity of purified Kinesin-1 in buffer, but similar to the speed of the motor in extracts (Blasius et al., 2007; Sung et al., 2008). In addition, we obtained mean values of 0.82±0.06 seconds for association time and 347±33 nm for run length. In *Pat1* mutant extracts, KHC-GFP also showed processive motility along microtubules, with approximately the same association time (0.74±0.07 seconds; n=771, P=0.43; Fig. 6C). However, velocity and run length were significantly reduced from those in wild-type extracts: by 20% and 42%, respectively (271±4 nm/second and 202±8 nm, respectively; P<0.001; Fig. 6D,E). A similar reduction in velocity was also observed in *Pat1* mutant extracts when MSD data for all trajectories were pooled and analyzed (control, 339±3 nm/second; *Pat1*, 246±4 nm/second; Fig. 6F). These results indicate that the velocity of Kinesin-1 is affected by loss of PAT1. A reduced efficiency of KHC motility in the absence of functional PAT1 could explain the mislocalization of *oskar* mRNA in mutant oocytes.

We conclude that PAT1 is important for the efficient trafficking of cargo by KHC along microtubules, and that the absence of PAT1 reduces the overall motility of KHC without affecting its microtubule-association time. These findings suggest that the requirement for PAT1 as a positive regulator of KHC-mediated transport relies on PAT1 function as a positive regulator of Kinesin motility.

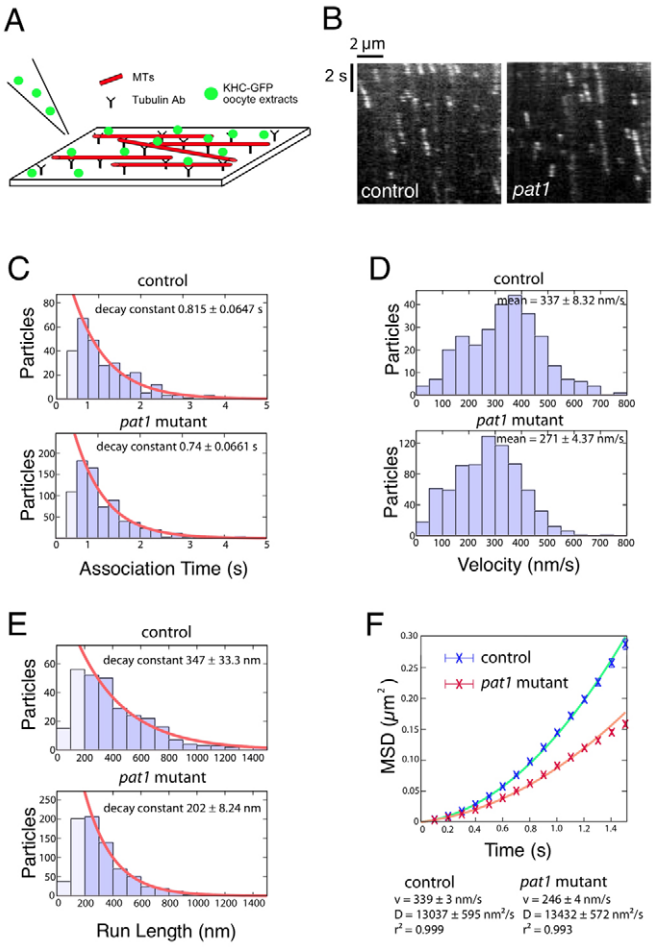

Fig. 6. The velocity and run length of Kinesin are reduced in the absence of *Pat1*. (**A**) The in vitro assay used to study the motility of KHC in control and *Pat1* ovarian extracts. KHC-GFP-expressing ovaries are dissected and added to immobilized Rhodamine-labeled microtubules in the presence of ATP. The motility of KHC is analyzed by TIRF microscopy, which allows single fluorophores close to the surface to be tracked when moving along an immobilized microtubule. (**B**) Representative kymographs of KHC in extracts that express tailless KHC-GFP, and that are either wild-type or mutant for *Pat1*. (**C-F**) The velocity and run length of KHC are reduced in *Pat1* mutants. (C-E) Bar charts of association time (C), velocity (D) and run length (E) of the individual KHC-GFP particles moving along microtubules in control and *Pat1* extracts (n=285 and n=771, respectively). Orange curves (C,E) represent fitting of the data (bins in darker blue) to exponential decays. (F) Mean square displacements (MSDs) calculated from the consolidated data were plotted against time intervals (t) and fitted with quadratic curves $MSD=v^2t^2+2Dt$ (v, velocity; D, diffusion coefficient). The velocity and run length of KHC are reduced by 20% and 42% in *Pat1* extracts, respectively. A statistically significant difference between control and *Pat1* extracts was seen in three independent experiments, although some variation occurred in the mean velocities. There was no significant difference in the diffusion coefficient (13,000±600 versus 13,400±600 nm²/second).

DISCUSSION

The localization of *oskar* mRNA and the anchoring of the nucleus by KHC are crucial for the establishment of the anterior-posterior and dorsal-ventral axes, respectively. KHC is also essential for the posterior localization of Dynein and for all ooplasmic movements. However, oocytes that lack KLC show no major defects in these KHC-dependent processes, suggesting that KHC binds these cargoes and is activated by a novel mechanism. Here, we investigate the molecular mechanism of Kinesin function in the germline using a combination of genetic, biochemical and motor-

tracking studies. We show that the KLC-like protein PAT1 interacts with Kinesin, functions in the transport of *oskar* mRNA and Dynein, and is required for the efficient motility of KHC along microtubules. We suggest that the role of PAT1 in the transport of cargoes in the cell correlates with PAT1 function as a positive regulator of Kinesin motility.

PAT1 is specifically required for *oskar* mRNA localization

Several lines of evidence suggest that the aberrant localization of *oskar* mRNA in *Pat1* mutants is due to defects in the transport of the transcript. PAT1 is not required for any other step in *oskar* mRNA biogenesis, as *Pat1* mutants do not affect its accumulation in the oocyte, its colocalization with Staufen or its translational regulation. Furthermore, the penetrance of the *oskar* mislocalization phenotype in *Pat1* mutants is weaker at later stages of oogenesis, suggesting that the transcript is not physically detaching and that its anchoring at the posterior is normal. PAT1 is also not required for the polarization of the oocyte or the microtubule cytoskeleton, nor for the Dynein-dependent localization of RNAs such as *bicoid*.

Taking into account the homology of PAT1 to the cargo-binding domain of KLC (the TPRs) and the biochemical interactions between PAT1 and Kinesin-1, one possible model for the function of PAT1 in *oskar* transport is that PAT1 contributes to the binding of the transcript to KHC. Whether PAT1 associates with *oskar* mRNA is unknown, but it is interesting to note that mammalian PAT1 interacts with zipcode-binding protein 1 (also known as Igf2bp1) (J. B. Dictenberg and R. H. Singer, personal communication), the *Drosophila* homolog of which, IMP, binds *oskar* mRNA and localizes to the posterior (Munro et al., 2006). However, oocytes lacking IMP localize *oskar* mRNA normally, indicating that the putative binding of PAT1 to IMP is not the only mechanism that would mediate the binding of PAT1 to the *oskar*-localizing complex.

Function of PAT1 and KLC in KHC-dependent transport

If PAT1 contributes to the binding of cargo to KHC, it is possible that, at least for some cargoes, it does so in conjunction with KLC. This hypothesis is supported by several findings. Firstly, PAT1 and KLC have a similar domain organization, with high sequence similarity in the KHC- and cargo-binding domains. Secondly, PAT1 and KLC form a complex with KHC. Lastly, Dynein seems to localize normally to the posterior in *Pat1* or *Klc* single mutants, but it accumulates at the anterior/lateral cortex when both genes are mutated, which is equivalent to the Dynein mislocalization phenotype observed in *Khc*-null mutant oocytes. These results suggest that PAT1 and KLC might redundantly mediate the interaction of Dynein with KHC that is required for its transport to the posterior.

This seems not to be the case for the transport of *oskar* mRNA to the posterior pole of the oocyte. Although the *oskar* mRNA mislocalization phenotype is more highly penetrant in *Pat1, Klc* double-mutant oocytes than in the single mutants, in contrast to *Khc* mutant oocytes, *oskar* mRNA is not found at the anterior/lateral cortex in these double mutants, but in the center and posterior of the oocyte. This suggests that PAT1 and KLC are not essential for KHC to bind *oskar* mRNA, and that other proteins must contribute to the interaction of *oskar* with the motor.

In contrast to the germline, where the absence of KLC results in no major defects in KHC-dependent processes, both *Khc* and *Klc* mutant larvae exhibit a neuronal phenotype in which axonal cargoes (e.g. synaptotagmin vesicles) accumulate in ‘clogs’ in the peripheral nerves (Hurd et al., 1996). Furthermore, *Khc* and *Klc* mutant larvae present locomotion defects, flip their posterior region upwards and paralyze progressively. Our preliminary data show that *Pat1* mutant axons also exhibit a high number of clusters of synaptotagmin vesicles (see Fig. S8 in the supplementary material), suggesting that PAT1 is also required for KHC function in the nervous system. However, *Pat1* mutants are viable and *Pat1* larvae show no obvious phenotypes. This indicates that Kinesin-1 has PAT1-independent functions that are important for locomotion and viability. In contrast to *Khc* and *Klc* mutants, the axonal clogs are not observed in the proximal region of the *Pat1* mutant peripheral nerves. This difference between *Pat1* and *Khc* or *Klc* larvae might explain the absence of paralysis and lethality in *Pat1* mutants. For further analysis of PAT1 function in the nervous system, it would be interesting to study whether the transport of molecules localized in a KLC-independent manner (e.g. FMRP or GRIP1) is disrupted in *Pat1* or *Pat1, Klc* double-mutant neurons.

In vertebrates there are two partially functionally overlapping KLC isoforms. The present study suggests that PAT1 might be a second KLC isoform in *Drosophila*. In light of our results it would be interesting to analyze whether KHC can form various complexes with PAT1 and with KLC. These distinct complexes could have overlapping, but not identical, specificities, providing a possible explanation for how one motor coordinates the transport of its many cargoes.

The velocity and run length of Kinesin are reduced in the absence of *Pat1*

In vitro motility assays using purified molecules are powerful systems to obtain mechanistic insights into the function of motors, but they might eliminate physiologically relevant factors that regulate their functions (Cai et al., 2007b; Sung et al., 2008). The use of KHC-GFP ovary extracts on defined microtubule tracks allowed us to analyze active KHC with and without PAT1 under more physiological conditions. Our results show that the velocity and run length of KHC, but not its association time, are reduced in the absence of PAT1. PAT1 is the first protein shown to positively regulate Kinesin speed and run length, without affecting its association time, revealing a novel mechanism of Kinesin regulation.

In light of the homology of PAT1 to the HR motif of KLC, and because PAT1 is found in a complex with KHC and KLC in co-immunoprecipitation experiments, a simple hypothesis for how PAT1 stimulates KHC motility is by direct physical interaction. Although we have detected interactions between *Drosophila* KLC and mammalian PAT1 in a yeast two-hybrid assay (data not shown), we have failed to detect a direct interaction between *Drosophila* KHC and PAT1 in this assay. This result suggests that either the PAT1 binding to KHC is transient and/or regulated by additional factors [e.g. KLC, as suggested by our results and those of Hammond et al. (Hammond et al., 2008)], or the hypothesis is incorrect and PAT1 does not directly bind KHC.

The mechanistic details of how PAT1 facilitates Kinesin-dependent transport would be the focus of future research. A potential mechanism for PAT1 to affect the motility of KHC is through the regulation of the KHC oligomerization state. To test this, the fluorescence intensity and pattern of fluorescence decay for each particle tracked were analyzed (Cai et al., 2007b) (see Fig. S7 in the supplementary material). Although GFP fluorescence fluctuates, we estimate that most particles contained one or two active GFP molecules, indicating that each particle primarily

contained a single dimer of KHC in both control and *Pat1* mutant extracts (see Fig. S7 in the supplementary material). Thus, the formation of higher-order oligomers is unlikely to account for the observed difference in velocity. Another possibility is that PAT1 affects Kinesin activity by binding microtubules, as PAT1 was identified in human cells as a weak microtubule-interacting protein (Zheng et al., 1998). However, we do not think this to be the case, as *Drosophila* PAT1 did not show a strong affinity for microtubules in sedimentation assays (data not shown).

What other mechanisms could account for the effect of PAT1 on Kinesin motility? One possibility is that PAT1 modulates KHC activity by acting on the motor domain. If we assume that PAT1 interacts with KHC via the stalk region, as is the case for KLC, how could this PAT1-KHC association act on the motor domain? Analysis of the KHC conformation changes revealed by FRET on cells confirmed that Kinesin-1 is partially folded while undergoing microtubule-based transport (Cai et al., 2007a; Coy et al., 1999; Friedman and Vale, 1999; Hisanaga et al., 1989; Verhey et al., 1998). This conformation would allow the stalk, and consequently PAT1, to come into close molecular contact with the neck and motor domains. Once in close contact, PAT1 could induce a change in the structure of the motor domain, for example by affecting the proximity between the two heads, so that they are in proper proximity for processive motility (Adio et al., 2009; Cai et al., 2007a), or by optimizing the internal tension required for the coordinated activity of the two heads (Hackney et al., 2003; Yildiz et al., 2008). It is also conceivable that the interaction of PAT1 with Kinesin releases an inhibitory mechanism of motor activity, as it has been shown for JIP1 (APLIP1) and UNC-76 (Blasius et al., 2007; Gindhart et al., 2003). In either case, these effects could be achieved directly by PAT1, or by an additional factor that is recruited to the motor in a PAT1-dependent manner, as has been described for the KHC-interacting protein Milton (Wang and Schwarz, 2009). Further biochemical and biophysical studies are needed to understand exactly how PAT1 achieves this novel regulation of KHC motility.

Whether PAT1 functions in both cargo binding and regulation of KHC motility is not clear. Genetic analyses suggest that PAT1 and KLC mediate the interaction of Dynein with KHC, as Dynein mislocalizes to the anterior/lateral cortex in a similar manner in *Pat1, Klc* double-mutant and *Khc* mutant oocytes (Brendza et al., 2000a; Brendza et al., 2002; Duncan and Warrior, 2002; Januschke et al., 2002; Palacios and St Johnston, 2002). In the case of *oskar* mRNA it is possible that the slower motility of KHC in the absence of PAT1 explains the mislocalization of this transcript in *Pat1* oocytes. This hypothesis is supported by several observations. Firstly, in contrast to components of the *oskar*-localization complex, PAT1 does not seem to accumulate at the posterior and is diffuse in the cytoplasm of the germline (see Fig. S9 in the supplementary material). Secondly, the absence of *Pat1* enhances the *oskar* mRNA mislocalization phenotype in oocytes expressing tailless KHC and it reduces the motility of this truncated motor. Thirdly, the *oskar* mRNA phenotype in *Pat1* mutants is similar to that of Khc^{17} and Khc^{23}, which are mutant alleles that result in a less motile KHC. In these alleles, *oskar* mRNA localizes to the posterior pole, but there is a small amount that accumulates in the middle of the oocyte (Serbus et al., 2005). It was subsequently shown that this is due to a delay in the transport of *oskar* mRNA (Zimyanin et al., 2007). This correlation between slowed motor mechanochemistry and ectopic *oskar* accumulation as a result of slowed *oskar* transport supports the hypothesis that the *oskar* phenotype in *Pat1* mutants is due to a slower KHC.

PAT1 was first identified in human cells, where it weakly interacts with microtubules and with APP. This work in human cells showed that PAT1 appears to regulate APP trafficking and processing, although the molecular mechanism of this regulation is not understood (Kuan et al., 2006; Zheng et al., 1998). Our results support a model in which the role of PAT1 in APP processing is probably linked to PAT1 function in regulating Kinesin. This hypothesis is further supported by recent work showing that mammalian PAT1 is required for the transport of mRNAs in neurons (J. B. Dictenberg and R. H. Singer, personal communication). Thus, the function of PAT1 as a novel regulator of Kinesin motility and cargo transport seems to be evolutionarily conserved.

Acknowledgements

We thank I. Davis, P. Lawrence and I. Alvarez-Garcia for comments on the manuscript; L. S. Goldstein, W. M. Saxton, H. Bellen, V. Mirouse, T. H. Hays, D. St Johnston and A. Ephrussi for their generous gifts of fly stocks, DNAs and antibodies; F. Severin, I. Kalaidzidis and M. Zerial for the introduction to the in vitro motility assays; A. Gardiol for helping with the larvae dissections; and Z. Cseresnyes for helping with imaging and motility analysis. We specially thank J. B. Dictenberg and R. H. Singer for discussions and sharing unpublished observations. P.L. and L.S.W. are supported by the Wellcome Trust, T.D is funded by the Biotechnology and Biological Sciences Research Council (BBSRC), M.M. is a Cancer Research UK Senior Research Fellow and I.M.P. is a Royal Society University Research Fellow. Deposited in PMC for release after 6 months.

Competing interests statement

The authors declare no competing financial interests.

Supplementary material

Supplementary material for this article is available at
http://dev.biologists.org/lookup/suppl/doi:10.1242/dev.048108/-/DC1

References

Adio, S., Jaud, J., Ebbing, B., Rief, M. and Woehlke, G. (2009). Dissection of kinesin's processivity. *PLoS ONE* **4**, e4612.

Blasius, T. L., Cai, D., Jih, G. T., Toret, C. P. and Verhey, K. J. (2007). Two binding partners cooperate to activate the molecular motor Kinesin-1. *J. Cell Biol.* **176**, 11-17.

Bowman, A. B., Kamal, A., Ritchings, B. W., Philp, A. V., McGrail, M., Gindhart, J. G. and Goldstein, L. S. (2000). Kinesin-dependent axonal transport is mediated by the sunday driver (SYD) protein. *Cell* **103**, 583-594.

Brendza, K. M., Rose, D. J., Gilbert, S. P. and Saxton, W. M. (1999). Lethal kinesin mutations reveal amino acids important for ATPase activation and structural coupling. *J. Biol. Chem.* **274**, 31506-31514.

Brendza, R. P., Serbus, L. R., Duffy, J. B. and Saxton, W. M. (2000a). A function for Kinesin I in the posterior transport of *oskar* mRNA and Staufen protein. *Science* **289**, 2120-2122.

Brendza, R. P., Sheehan, K. B., Turner, F. R. and Saxton, W. M. (2000b). Clonal tests of conventional kinesin function during cell proliferation and differentiation. *Mol. Biol. Cell* **11**, 1329-1343.

Brendza, R. P., Serbus, L. R., Saxton, W. M. and Duffy, J. B. (2002). Posterior localization of dynein and dorsal-ventral axis formation depend on kinesin in Drosophila oocytes. *Curr. Biol.* **12**, 1541-1545.

Cai, D., Hoppe, A. D., Swanson, J. A. and Verhey, K. J. (2007a). Kinesin-1 structural organization and conformational changes revealed by FRET stoichiometry in live cells. *J. Cell Biol.* **176**, 51-63.

Cai, D., Verhey, K. J. and Meyhofer, E. (2007b). Tracking single Kinesin molecules in the cytoplasm of mammalian cells. *Biophys. J.* **92**, 4137-4144.

Chou, T. B. and Perrimon, N. (1996). The autosomal FLP-DFS technique for generating germline mosaics in Drosophila melanogaster. *Genetics* **144**, 1673-1679.

Chou, T.-B., Noll, E. and Perrimon, N. (1993). Autosomal P[ovo^{D1}] dominant female-sterile insertions in *Drosophila* and their use in generating germ-line chimeras. *Development* **119**, 1359-1369.

Clark, I., Giniger, E., Ruohola-Baker, H., Jan, L. Y. and Jan, Y. N. (1994). Transient posterior localization of a kinesin fusion protein reflects anteroposterior polarity of the Drosophila oocyte. *Curr. Biol.* **4**, 289-300.

Coy, D. L., Hancock, W. O., Wagenbach, M. and Howard, J. (1999). Kinesin's tail domain is an inhibitory regulator of the motor domain. *Nat. Cell Biol.* **1**, 288-292.

Diefenbach, R. J., Mackay, J. P., Armati, P. J. and Cunningham, A. L. (1998). The C-terminal region of the stalk domain of ubiquitous human kinesin heavy chain contains the binding site for kinesin light chain. *Biochemistry* **37**, 16663-16670.

Duncan, J. E. and Warrior, R. (2002). The cytoplasmic Dynein and Kinesin motors have interdependent roles in patterning the Drosophila oocyte. *Curr. Biol.* **12**, 1982-1991.
Friedman, D. S. and Vale, R. D. (1999). Single-molecule analysis of kinesin motility reveals regulation by the cargo-binding tail domain. *Nat. Cell Biol.* **1**, 293-7.
Gauger, A. K. and Goldstein, L. S. (1993). The Drosophila kinesin light chain. Primary structure and interaction with kinesin heavy chain. *J. Biol. Chem.* **268**, 13657-13666.
Gindhart, J. G., Jr, Desai, C. J., Beushausen, S., Zinn, K. and Goldstein, L. S. (1998). Kinesin light chains are essential for axonal transport in Drosophila. *J. Cell Biol.* **141**, 443-454.
Gindhart, J. G., Chen, J., Faulkner, M., Gandhi, R., Doerner, K., Wisniewski, T. and Nandlestadt, A. (2003). The kinesin-associated protein UNC-76 is required for axonal transport in the Drosophila nervous system. *Mol. Biol. Cell* **14**, 3356-3365.
Hackney, D. D., Stock, M. F., Moore, J. and Patterson, R. A. (2003). Modulation of kinesin half-site ADP release and kinetic processivity by a spacer between the head groups. *Biochemistry* **42**, 12011-12018.
Hammond, J. W., Griffin, K., Jih, G. T., Stuckey, J. and Verhey, K. J. (2008). Co-operative versus independent transport of different cargoes by Kinesin-1. *Traffic* **9**, 725-741.
Helenius, J., Brouhard, G., Kalaidzidis, Y., Diez, S. and Howard, J. (2006). The depolymerizing kinesin MCAK uses lattice diffusion to rapidly target microtubule ends. *Nature* **441**, 115-119.
Hisanaga, S., Murofushi, H., Okuhara, K., Sato, R., Masuda, Y., Sakai, H. and Hirokawa, N. (1989). The molecular structure of adrenal medulla kinesin. *Cell Motil. Cytoskeleton* **12**, 264-272.
Hoepfner, S., Severin, F., Cabezas, A., Habermann, B., Runge, A., Gillooly, D., Stenmark, H. and Zerial, M. (2005). Modulation of receptor recycling and degradation by the endosomal kinesin KIF16B. *Cell* **121**, 437-450.
Hurd, D. D., Stern, M. and Saxton, W. M. (1996). Mutation of the axonal transport motor kinesin enhances paralytic and suppresses Shaker in Drosophila. *Genetics* **142**, 195-204.
Hutterer, A., Glotzer, M. and Mishima, M. (2009). Clustering of centralspindlin is essential for its accumulation to the central spindle and the midbody. *Curr. Biol.* **19**, 2043-2049.
Januschke, J., Gervais, L., Dass, S., Kaltschmidt, J. A., Lopez-Schier, H., Johnston, D. S., Brand, A. H., Roth, S. and Guichet, A. (2002). Polar transport in the Drosophila oocyte requires Dynein and Kinesin I cooperation. *Curr. Biol.* **12**, 1971-1981.
Kuan, Y. H., Gruebl, T., Soba, P., Eggert, S., Nesic, I., Back, S., Kirsch, J., Beyreuther, K. and Kins, S. (2006). PAT1a modulates intracellular transport and processing of amyloid precursor protein (APP), APLP1, and APLP2. *J. Biol. Chem.* **281**, 40114-40123.
Littleton, J. T., Bellen, H. J. and Perin, M. S. (1993). Expression of synaptotagmin in Drosophila reveals transport and localization of synaptic vesicles to the synapse. *Development* **118**, 1077-1088.
Markussen, F. H., Michon, A. M., Breitwieser, W. and Ephrussi, A. (1995). Translational control of oskar generates short OSK, the isoform that induces pole plasma assembly. *Development* **121**, 3723-3732.
McGrail, M. and Hays, T. S. (1997). The microtubule motor cytoplasmic dynein is required for spindle orientation during germline cell divisions and oocyte differentiation in Drosophila. *Development* **124**, 2409-2419.
Micklem, D. R., Dasgupta, R., Elliott, H., Gergely, F., Davidson, C., Brand, A., Gonzalez-Reyes, A. and St Johnston, D. (1997). The mago nashi gene is required for the polarisation of the oocyte and the formation of perpendicular axes in Drosophila. *Curr. Biol.* **7**, 468-478.
Munro, T. P., Kwon, S., Schnapp, B. J. and St Johnston, D. (2006). A repeated IMP-binding motif controls oskar mRNA translation and anchoring independently of Drosophila melanogaster IMP. *J. Cell Biol.* **172**, 577-588.
Nielsen, E., Severin, F., Backer, J. M., Hyman, A. A. and Zerial, M. (1999). Rab5 regulates motility of early endosomes on microtubules. *Nat. Cell Biol.* **1**, 376-382.
Okada, Y. and Hirokawa, N. (1999). A processive single-headed motor: kinesin superfamily protein KIF1A. *Science* **283**, 1152-1157.
Palacios, I. M. and St Johnston, D. (2002). Kinesin light chain-independent function of the Kinesin heavy chain in cytoplasmic streaming and posterior localisation in the Drosophila oocyte. *Development* **129**, 5473-5485.
Rice, S. E. and Gelfand, V. I. (2006). Paradigm lost: milton connects kinesin heavy chain to miro on mitochondria. *J. Cell Biol.* **173**, 459-461.
Serbus, L. R., Cha, B. J., Theurkauf, W. E. and Saxton, W. M. (2005). Dynein and the actin cytoskeleton control kinesin-driven cytoplasmic streaming in Drosophila oocytes. *Development* **132**, 3743-3752.
St Johnston, D., Beuchle, D. and Nusslein-Volhard, C. (1991). Staufen, a gene required to localize maternal RNAs in the Drosophila egg. *Cell* **66**, 51-63.
Sung, H. H., Telley, I. A., Papadaki, P., Ephrussi, A., Surrey, T. and Rorth, P. (2008). Drosophila ensconsin promotes productive recruitment of Kinesin-1 to microtubules. *Dev. Cell* **15**, 866-876.
van Eeden, F. J., Palacios, I. M., Petronczki, M., Weston, M. J. and St Johnston, D. (2001). Barentsz is essential for the posterior localization of oskar mRNA and colocalizes with it to the posterior pole. *J. Cell Biol.* **154**, 511-523.
Verhey, K. J., Lizotte, D. L., Abramson, T., Barenboim, L., Schnapp, B. J. and Rapoport, T. A. (1998). Light chain-dependent regulation of Kinesin's interaction with microtubules. *J. Cell Biol.* **143**, 1053-1066.
Verhey, K. J., Meyer, D., Deehan, R., Blenis, J., Schnapp, B. J., Rapoport, T. A. and Margolis, B. (2001). Cargo of kinesin identified as JIP scaffolding proteins and associated signaling molecules. *J. Cell Biol.* **152**, 959-970.
Wang, X. and Schwarz, T. L. (2009). The mechanism of Ca^{2+}-dependent regulation of kinesin-mediated mitochondrial motility. *Cell* **136**, 163-174.
Yildiz, A., Tomishige, M., Gennerich, A. and Vale, R. D. (2008). Intramolecular strain coordinates kinesin stepping behavior along microtubules. *Cell* **134**, 1030-1041.
Zheng, P., Eastman, J., Vande Pol, S. and Pimplikar, S. W. (1998). PAT1, a microtubule-interacting protein, recognizes the basolateral sorting signal of amyloid precursor protein. *Proc. Natl. Acad. Sci. USA* **95**, 14745-14750.
Zimyanin, V., Lowe, N. and St Johnston, D. (2007). An oskar-dependent positive feedback loop maintains the polarity of the Drosophila oocyte. *Curr. Biol.* **17**, 353-359.
Zimyanin, V. L., Belaya, K., Pecreaux, J., Gilchrist, M. J., Clark, A., Davis, I. and St Johnston, D. (2008). In vivo imaging of oskar mRNA transport reveals the mechanism of posterior localization. *Cell* **134**, 843-853.